Optimization of Cooling Fan Based on Unequal Angle and Leading-Edge Triangle Blade Design

Xie Youfu and Jiang Feng

Bosch Automotive Systems (Wuxi) Ltd. E-mail: youfu.xie@cn.bosch.com

(Received 7 December 2023; accepted 25 July 2024)

In order to reduce the noise of the axial fan, an uneven blade spacing was used to optimize tonal noise and blade leading edge triangles were added to optimize the broadband noise. First, different angular distribution schemes were designed on the basis of ensuring the dynamic balance of the fan, and the noise of the different schemes was simulated by using the computational aeroacoustics (CAA) numerical simulation method. Then, the best optimal angular distribution design was selected for experimental verification, which confirmed the reliability of the numerical calculation. The test results also show that the uneven blade spacing has little effect on the fan pressure and efficiency. Additionally, triangular leading edges were added to each blade based on the uneven blade spacing design. Combining these two optimization schemes proved to reduce the fan noise by 13.4 dBA.

NOMENCLATURE

Acronym

BPF	Blade passing frequency
CAA	Computational Aeroacoustics
SPL	Sound pressure level
FW-H	Ffowcs-Williams-Hawkings
NVH	Noise, vibration, and harshness

Greek

α_i	Blade spacing angle
π	Circle ratio
ρ	Density
$\delta(f)$	Dirac generalized function
μ	Viscosity

Roman

N	Order
n	Number of blades
R	Fan speed in rpm
j	Serial number of blades
A	Phase modulation angle
s	Number of groups
t	Time
c_0	Speed of sound
e_{ij}	Viscous stress tensor
P	Air pressure
T_{ij}	Lighthill tensor
u	Velocity component
x	Spatial coordinate components
V_n	Normal velocity component
L_i	Blade wall load components
$H(f)$	Heaviside's generalized function

Subscript

i	No.
j	No.
n	Normal

1. INTRODUCTION

Fan noise is usually characterized by discrete and broadband noise. Discrete noise is caused by periodic fluctuations in blade loading and is usually dominated by the BPF and its higher harmonic tones. Therefore, it is also known as tonal noise. The broadband component originates from the separated flow in the impeller and is distributed over a wide frequency range in the noise spectrum. A great deal of research has been conducted on fans to reduce the overall noise level by reducing both components.

As early as 1967, Lowson first proposed the idea of using circumferentially randomized blades to reduce rotor discrete noise.[1] It was first theoretically investigated and theoretically proven by Mellin and Sovran in 1970.[2] Based on this, Enwald et al.[3] proposed a sinusoidal modulation method for rearranging the blade spacing of an axial fan rotor; this method reshaped the noise spectrum without causing any undesirable mechanical imbalance or aerodynamic losses, and they achieved a reduction in the fundamental frequency noise of 8 dB by using a 22-blade axial fan. In 1986, Sun XF derived the sound radiation formula of an uneven fan through S.E. Wright's BLH-theory[4] and proved through testing that unequal pitch arrangement can effectively reduce the noise up to 10.67 dB, and also verified that the angle change rate within 20% will not have a large impact on the efficiency and air volume.[5] Recently, unevenly arranged fans have been studied more and more extensively, based on S. Lewy's research,[6] a random modulation method was proposed as an alternative method, and demonstrated good results.[7,8]

The use of the unequal spacing arrangement method can effectively reduce the order noise when the total sound pressure level reduction is limited. As a result, the industry for the fan's vortex noise proposed the front bend and changed the line of thinking to effectively reduce the broadband noise.[9] Ouyang[10] using the forward-skewed blade design and the results have shown a great improvement of aerodynamic and acoustic performance. Cai Na[11] found that the aerodynamic noise of the curved swept blade fan was always lower than that of the radial blade fan by about 4 dB in all flow ranges of variable conditions, and the noise was reduced in the whole wide frequency band. Boyan Jiang[12] combined the unevenly spaced blades and

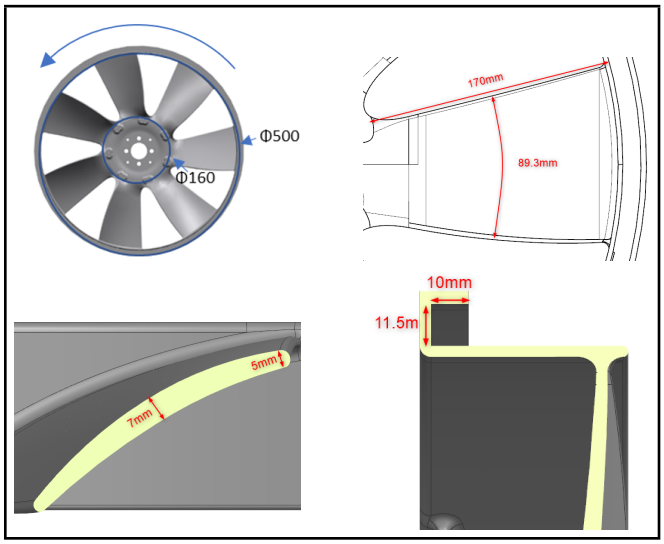

Figure 1. Fan structure.

the forward-curved-blades design which showed that a reasonable blade distribution designed by this method could reduce tonal noise without negatively affecting the aerodynamic performance and the overall noise level.

In recent years, more studies have been proposed. Mehdi Yadegari. et al.[13] explored the use of perforated surfaces as an innovative method for noise reduction. Lai, Y. et al.[14] investigated how different installation setups (free field, wall mounted, and in-vehicle) affect fan noise.

In this study, the optimization of noise is carried out by designing the blade angle using the sinusoidal modulation method as well as through adding a triangle in front of the blades to achieve the forward curvature design. Then, the verification of the design will be completed by both acoustic simulation and experimental validation.

2. FAN NOISE ANALYSIS

2.1. Fan Structure

As shown in Fig. 1, the axial fan is a 7-blade double curved blade type with a diameter of 500 mm, a hub diameter of 160 mm, average chord length 89.3 mm, blade length 170 mm, average thickness 6 mm, a C-shaped wind protection ring structure, anticlockwise rotation with a rated speed of 2500 rpm and a blade tip speed of 0.2 Ma.

2.2. Noise Testing

Figure 2 is the structure of the Thermal Management System (TMS) which includes radiator, motor, fan and brackets. Testing was done in a semi-anechoic chamber with an ambient noise level of 38.0 dB. According to industry specifications, the noise measurement point needs to be one meter to the side, so a microphone was installed 1 meter to the side of the cooling fan for testing. This was arranged as shown in Fig. 3, 1 m from the radiator frame and 0.75 m in height from the ground.

LMS test equipment as well as PCB microphones were used for testing, with a sampling frequency of 20480 Hz. Testlab software was used for data processing, with the FFT method to convert the time domain data to frequency domain data, using the Hanning Window Function, with a frequency resolution of 1 Hz and A-weighting, to obtain the spectral data as well as the RMS value of the sound pressure level.

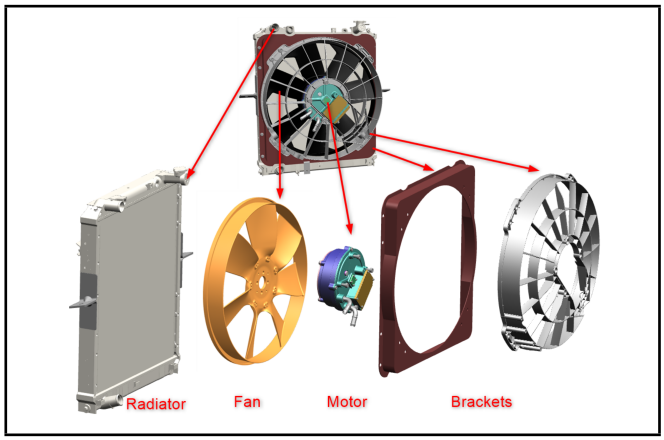

Figure 2. TMS structure.

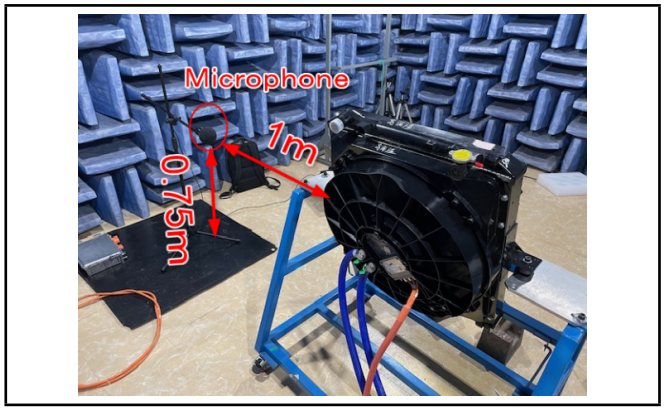

Figure 3. Noise Test.

In order to confirm the influence of the radiator and grille on the noise, a TMS, a TMS without radiator, a TMS with simplified metal bracket were tested separately.

Table 1 shows the noise results at different speeds, they are very close, with a maximum deviation of 0.5 dB, so the grille and heat sink have a relatively small effect on the overall noise level.

The analyses in the following sections are based on the TMS test result, 98.0 dBA at 2500 rpm.

2.3. Fan Aerodynamic Noise Analysis

2.3.1. Analyzing fan blade passing noise

The formula for N-th order of BPF (blade passage frequency) is:

$$BPF = N \cdot n \cdot R/60; \tag{1}$$

where, n is the number of blades, R is the fan speed in RPM, N is the harmonic number and is taken as a positive integer. The base BPF frequency of a 7-blades fan at 2500 rpm is:

$$BPF_1 = 1 \cdot 7 \cdot 2500/60 = 291.7 \text{ Hz}. \tag{2}$$

Table 1. Comparison of different test samples.

RPM	TMS	TMS without radiator	TMS without grill (instead of simplified metal bracket)
1000	73.3 dBA	73.4 dBA	73.1 dBA
1500	83.5 dBA	83.9 dBA	83.6 dBA
2000	91.1 dBA	91.6 dBA	91.5 dBA
2500	98.0 dBA	98.3 dBA	97.9 dBA

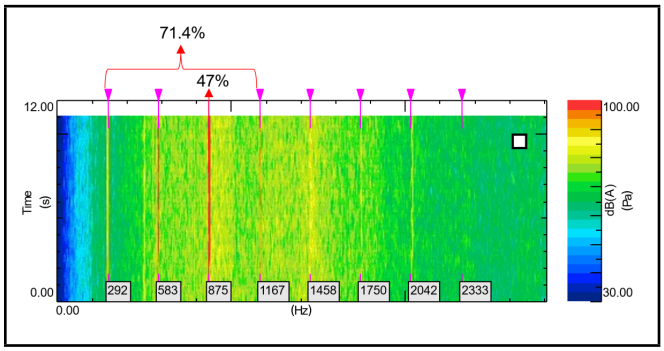

Figure 4. Waterfall diagram of the noise spectrum.

2.3.2. Analyze the noise spectrum data of the fan at 2500 rpm.

From the test data in Fig. 4, it can be concluded that the noise energy is mainly concentrated in the frequencies of 292/583/875/1167 Hz, and the order frequency coincides with the calculated BPF order frequency.

3. OPTIMIZATION OF BPF NOISE

3.1. Reduce BPF Noise

The BPF belongs to the discrete noise that occurs as a result of periodically induced non-stationary forces, and its frequency is mainly related to the blade speed and the number of blades.

As the fan is uniformly arranged, when the fan rotates, the blades periodically cut the air, which will cause the blades to beat the air uniformly according to the number of times the blades are counted in each rotational cycle, thus forming BPF noise.

A number of technical means have been proposed to reduce the tonal noise of cooling fans. The most important design method is the uneven arrangement of the blades.

3.2. Optimization of Uneven Blades Arrangement

The design of uneven blades mainly considers two aspects of the constraints, one is the blade arrangement changes, which allows for meeting the dynamic balance conditions of the impeller operation; and the second is the angle between the blades cannot be too large, otherwise the aerodynamic performance of the fan may cause large changes.

When considering the static and dynamic balance of the fan, the angles between the 7-blade fan α_i need to satisfy the Eq. (3) as seen below:

$$\begin{cases} \sum_{j=1}^{7} \cos\left(\sum_{i=1}^{j} \alpha_i\right) = 0 \\ \sum_{j=1}^{7} \sin\left(\sum_{i=1}^{j} \alpha_i\right) = 0 \\ \sum_{i=1}^{7} \alpha_i = 360^\circ \end{cases} \cdot \tag{3}$$

Since the constraints can be solved by an infinite set of solutions, the clamping angle between the blades is modulated by a blade grouping self-modulation scheme, which groups the seven blades and sets the phase modulation angle for each group of clamping angles. According to the company's historical product development experience, the grouping and phase modulation angles need to satisfy the Eq. (4):

Table 2. Comparison of perspectives of different optimization scenarios.

Angle	Uneven1	Uneven2	Uneven3	Uneven4
Phase	3.3	4.5	6.7	8.6
1	53.5	55.90	58.7	59.8
2	50	45.0	40.9	39.3
3	46	49.8	48.8	48.4
4	61	58.6	63.1	64.9
5	46	49.8	48.8	48.4
6	50	45	40.9	39.3
7	53.5	55.9	58.7	59.8

$$\alpha_{j+1} = j \cdot \frac{2\pi}{n} + ASin\left(s\sum_{i=1}^{j}\alpha_i\right) - \alpha_j; \tag{4}$$

where n is the number of blades, A is the phase modulation angle, and s is the number of groups.

Since the number of blades is 7, and according to experience, the number of groups is set to 2. Considering the impact on the aerodynamic performance of the fan and according to experience, the phase modulation angle takes the value of 0–10°. In order to study the difference of the angle between different phase modulation angles, a total of four groups of different angles are taken for simulation and comparison.

3.3. Validating Optimization Schemes

CAA refers to Computational Aeroacoustics, which is a cross-cutting and marginal discipline between aerodynamics and acoustics, and mainly studies the generation mechanism, propagation of aerodynamic noise caused by gas flow and its interaction with objects.

One of the first outstanding theoretical contributions to modern aerodynamic acoustics was the fruitful work of Lighthill[15] in the 1950's. Lighthill developed the theory of acoustic modelling. Lighthill's equations can be derived from the fundamental equations of fluid dynamics, the N-S equation, and the continuity equation. By differentiating the continuity equation with respect to t and taking the divergency of the momentum equation, respectively, and subtracting the results, the Lighthill equation is given:

$$\frac{\partial^2 \rho'}{\partial t_2} - c_0^2 \nabla^2 \rho' = \frac{\partial^2 T_{ij}}{\partial x_i \partial x_j}; \tag{5}$$

where, $\rho' = \rho - \rho_0$, it is the fluid density fluctuations, T_{ij} is the Lighthill stress tensor. $T_{ij} = \rho u_i u_j - e_{\mathrm{ij}} + \delta_{ij}(p - c_0^2\rho)$ is the Lighthill stress tensor e_{ij} is the viscous stress tensor, and,

$$e_{\mathrm{ij}} = \mu\left(\frac{\partial u_i}{\partial x_j} + \frac{\partial u_j}{\partial x_i} - \frac{2}{3}\delta_{\mathrm{ij}}\frac{\partial u_i}{\partial x_i}\right); \tag{6}$$

The Lighthill equation is obtained under the assumption of free space, Ffowcs Williams&Hawking discussed the acoustic radiation of an object in arbitrary motion, and applied the generalized Green's function method to consider the problem of sound emission at the boundary of a solid moving in a fluid, and based on Lighthill's equation, the FW-H[16] acoustic propagation equation is derived:

$$\frac{1}{a^2}\frac{\partial^2 p'}{\partial t^2} - \frac{\partial^2 p'}{\partial x_i^2} = \frac{\partial}{\partial t}\left[\rho_* V_n \delta(f)\right] - \frac{\partial}{\partial x_i}\left[L_i \delta(f)\right] + \frac{\bar{\partial}^2}{\partial x_i x_j}\left[T_{ij} H(f)\right]. \tag{7}$$

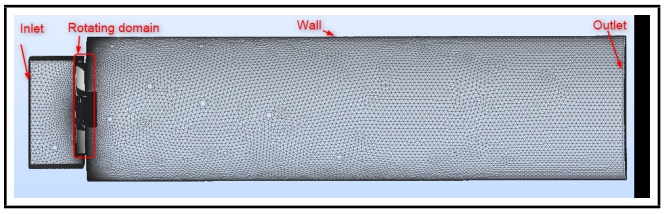

Figure 5. CFD simulation model.

The first term on the right-hand side of the FW-H equation is a monopole source due to the periodic rotation of the blade (mass/thickness source term); the second term is a dipole source due to the force acting on the fluid at the surface of the object (force pulsation source term); and the third term is a dipole and quadrupole source due

to the change in volume caused by the displacement of the object (stress pulsation source term).

3.4. Simulation Model

A hybrid approach is used to predict the radiated noise in the free field. The transient flow field around the fan blade is first accurately simulated based on CFD analysis to obtain its surface pressure data, and then the radiated noise of the fan blade is predicted using the CAA method.

Figure 5 is the CFD model of the fan, which has a total of 78722314 elements and a minimum element size of 0.2 mm. Considering the convergence of the numerical calculation, the inlet is selected as a square area with reference to the structure of the radiator. The outlet is a cylindrical area, the medium in the simulation model basin is flowing air, the total pressure of the inlet and outlet is relative to the atmospheric pressure, and there is no additional pressure in the inlet and outlet, and the atmospheric pressure is given as 0 Pa. The inlet and outlet are both set to be the pressure inlet and outlet, and other places are set to be the wall. The fan blade is set as a moving wall condition with zero rotational speed with respect to the rotating domain. The rotating domain is set as an air fluid, and when the rotating domain rotates at 2500 rpm, it drives the fan to rotate at this speed. The steady state operation is performed based on the RNG k -e turbulence model using Ansys Fluent software, and the transient operation is performed using the Large Eddy simulation (LES) model after convergence. The total number of grids is close to 80 million, meeting the LES calculation requirements. The time for the fan to make one revolution at 2500 rpm is 0.024 s, so the step time of transient simulation was set to 0.000133 s, and export 600 steps.

Figure 6 is the CAA simulation model using ACTRAN, including the fan rotation region, the dynamic-static interface sound source region, the body sound source region, the sound propagation region, and the monitoring microphone.

The noise source generated by fan rotation is integrated into the dynamic-static interface of the fan as well as the region of the body sound source. Then, the sound propagation is calculated to monitor the sound pressure at the specified point (1 m at the side).

3.5. Validation of the Simulation Method

Comparing the simulation results of the fan with the test data, the spectrum is shown in Fig. 7.

The blue curve is the test data, the noise overall value is 98.0 dBA, and the red curve is the simulation data, the noise

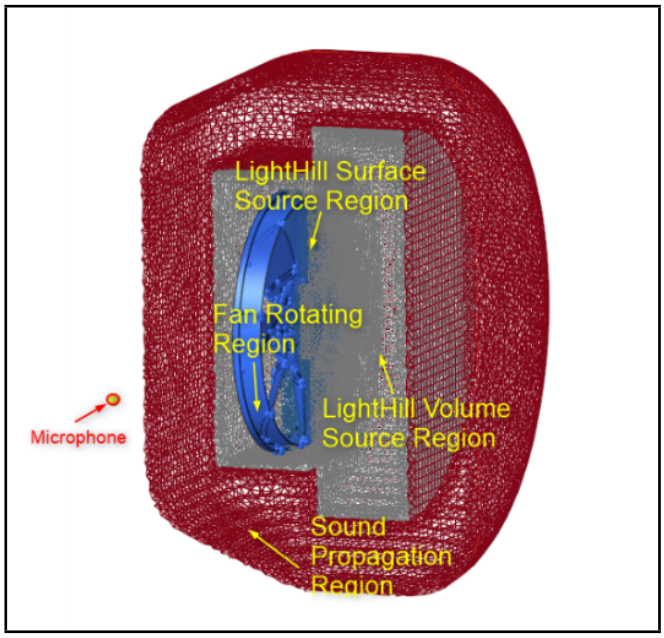

Figure 6. CAA simulation model.

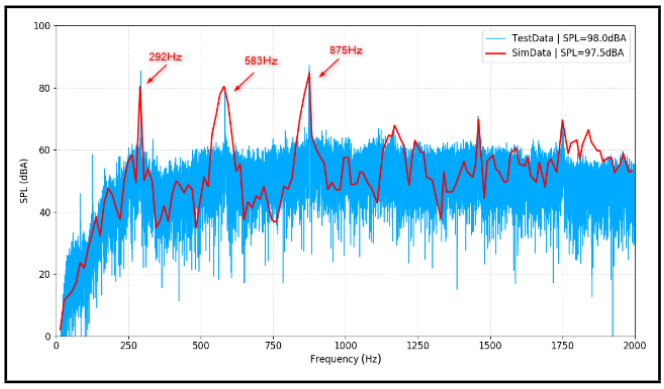

Figure 7. Comparison of simulation and test data.

OA value is 97.5 dBA, which is 0.5 dB different from the test value, and the error is within the acceptable range (±3 dB). The peaks corresponding to the order noise coincide with the test data.

3.6. Uneven Spaced Simulation

Comparing the simulation results in Fig. 8 of four different designs, it is found that Uneven3, with the lowest noise (green curve) at a phase modulation angle of 6.7°, is 90.1 dB. This is 7.4 dB lower than that of the original uniformly arranged design and eliminates the obvious order noise and also effectively reduces the peak value.

3.7. Test

In order to validate the optimized uneven design, test of Uneven3 was carried out on prototype.

The test result is 90.7 dBA, with a 7.3 dB decrease at 2500 rpm at rated operating conditions. Analyzing the spectrum at 2500 rpm.

As shown in Fig. 10, the results of spectral analysis show that the uneven arrangement design reduces the fan noise by 7.3 dB.

The fan efficiency is the ratio of the fan flow rate multiplied by pressure to fan input power. Based on ISO 5801:2017,[17]

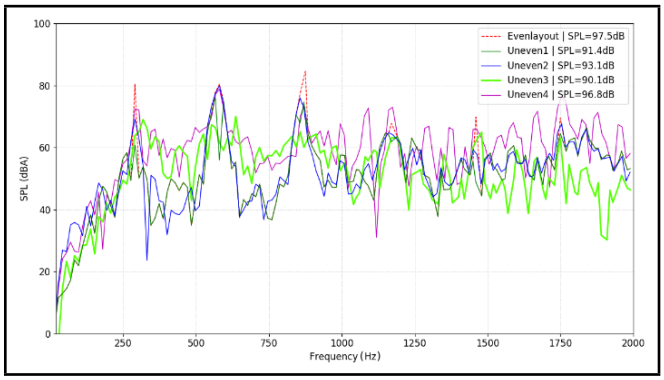

Figure 8. Comparison of uneven arrangement scheme and uniform arrangement scheme.

Figure 9. Uneven3 prototype.

Fig. 11 shows the efficiency test conducted in a wind tunnel where both the inlet and outlet areas are free boundaries. Table 3 shows the air pressure and efficiency comparison results.

The test results show that the fan efficiency and heat dissipation capacity of the uneven blade arrangement design are less affected compared to the uniform arrangement design, confirming that the scheme is feasible in optimizing the BPF noise.

4. OPTIMIZATION OF FAN VORTEX NOISE

4.1. Generation Mechanism of Broadband Vortex Noise

Broadband vortex noise is mainly caused by the random pulsation force acting on the blade. When the airflow flows through the blades, it generates turbulent surface layers and vortices, which cause pressure pulsations on the blades. This pulsation is obviously chaotic and irregular, and thus this noise has a wide frequency range.

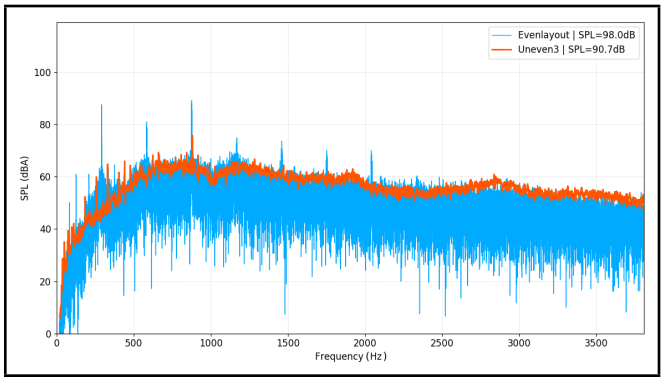

Figure 10. Comparison of 2500 RPM test spectra of uneven and uniform samples.

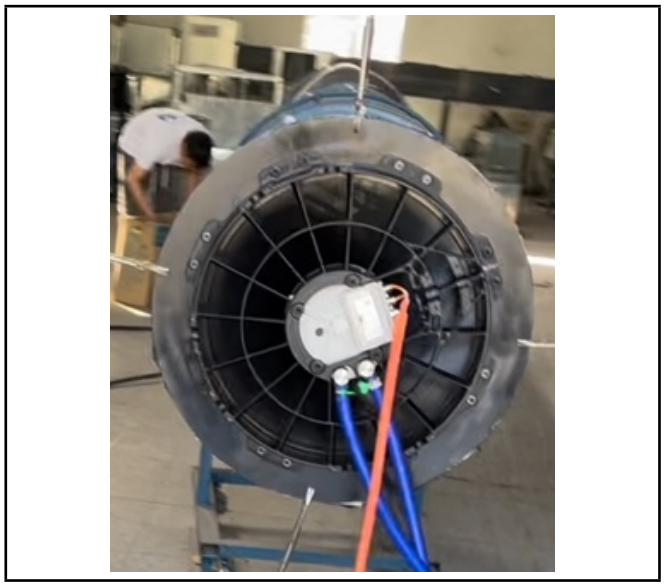

Figure 11. Efficiency test in a wind tunnel.

Table 3. Comparison of fan performance test between uniform and uneven samples.

Parametric	Uniform	Uneven design
Capacity	2.75 m^3/s	2.73 m^3/s
Static Pressure	501 Pa	497 Pa
Efficiency	53.1%	53.0%

4.2. Blade Optimization

To reduce the fan vortex noise, an effective method is to add triangular to the leading edge of the fan blade, it is a reasonable approach as it minimally disrupts the blade profile while effectively reducing noise.

The size of the triangle is the main factor affecting the optimization result of the blade. Considering the impact on the aerodynamic layout of the original airfoil after increasing the triangle area, the height of the triangle needs to be controlled within a certain range, as well as the width. Therefore, on the basis of the uneven arrangement scheme, the four sets of triangle dimensions in Table 4 are defined empirically for analysis, and the optimal values are taken to improve the design.

4.3. CFD Analysis Results

The left picture in Fig. 13 shows the CFD results of the original design. The streamlines are more concentrated in the tip area, generating local vortices. The right picture shows the CFD results of the design with an added leading-edge triangle.

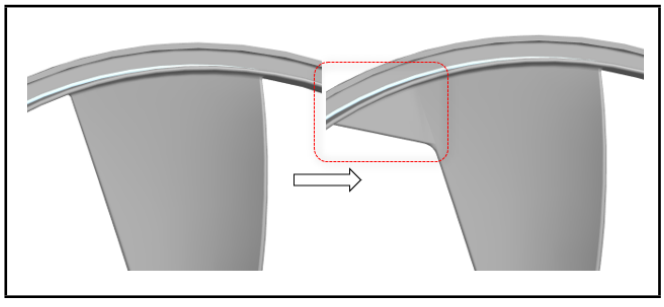

Figure 12. Add Leading edge Triangle.

Table 4. Different forward bending scenarios.

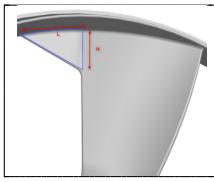

Triangular	Triangle 1	Triangle 2	Triangle 3	Triangle 4
L (mm)	30	40	50	60
H (mm)	50	60	30	40

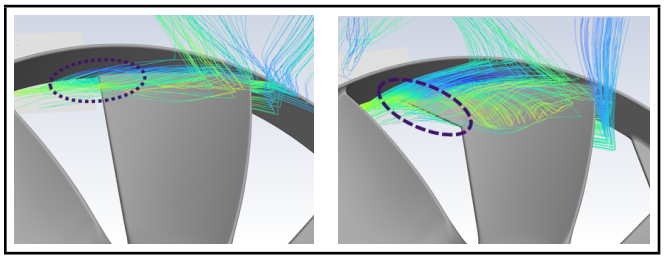

Figure 13. Comparison of CFD streamline results.

The streamlines are dispersed over the entire triangular edge, and the energy is dispersed resulting in fewer vortices.

4.4. Acoustic Simulation Results

A comparison of the CAA calculation results is shown in Fig. 14:

The results show that Triangle 4 (green widening curve) with a triangle width of 60 mm and height of 40 mm has the lowest noise. The fan rated noise at 2500 rpm was 84.2 dB, which was reduced to below the design target of 85 dB.

4.5. Test Validation

In order to verify the optimized leading-edge triangle based on uneven design, the sample part was tested.

The test results show that the noise decreases at all speeds compared to the original uneven arrangement scheme, and the noise is 84.6 dBA at 2500 rpm at rated condition, a decrease of 6.1 dB compared to the uneven arrangement scheme, and a decrease of 13.4 dB compared to the original uniform arrangement scheme.

The comparison of the spectral data is as Fig. 16, from which it can be seen that the uneven arrangement + forward curvature scheme (green curve) has a significantly lower noise level over the whole wide band than the scheme designed for uneven arrangement only, which proves that the optimized design scheme is effective and achieves the design objectives.

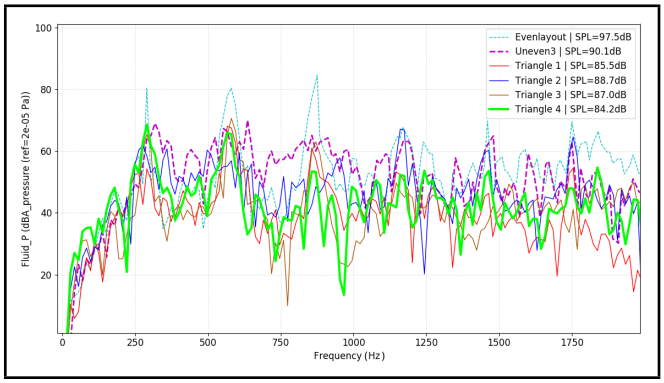

Figure 14. Comparison of model simulation results for different forward bending scenarios.

Figure 15. Test sample of the optimal leading triangle and uneven arrangement design.

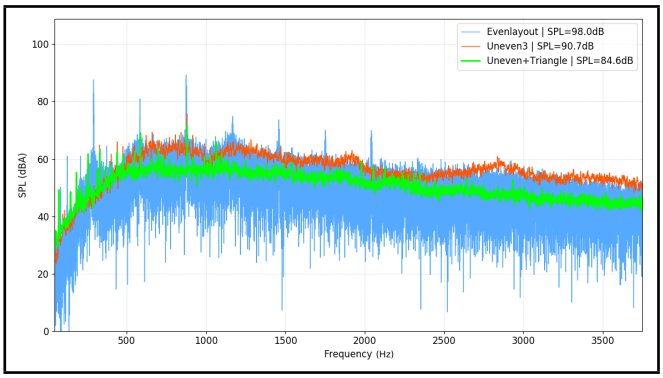

Figure 16. Comparison of test spectra for uneven arrangement + forward bending scheme.

To verify the effect of the optimized design on fan efficiency, it was tested, and the comparison results are shown in the Table 5.

The results show that due to the front bend increasing the effective area of the fan resulting in a slight increase in both wind pressure and air volume, the efficiency is 0.6% higher than the initial scheme. This proves that the scheme is not only effective in reducing the noise of the fan, but also has an increase on the efficiency.

Aerodynamic noise, as the focus of NVH research, has many influencing factors, system complexity and a certain degree of randomness, and has always been the focus of the project in the related product development process. At the same time, in the field of fan noise, scholars and enterprises have also conducted a lot of research and proposed many solutions from different perspectives, such as the widely used bionic blade design[18–20] in the fields of aerospace engines and other fields. The next step will be to continue research in this area.

5. SUMMARIES

Through numerical simulation and experimental verification, the uneven arrangement of the fan effectively reduced the noise of 2500 rpm of the rated condition of the fan by 7.3 dB. The unevenly arranged blades and leading triangle design effectively reduced the fan noise at 2500 rpm by 13.4 dB under the premise of ensuring the performance of the fan, which

Table 5. Comparison of performance test for uneven arrangement + leading Triangle scheme.

parametric	Equal	Unequal	Uneven + Triangle
air volume	2.75 m^3/s	2.73 m^3/s	2.76 m^3/s
static pressure	501 Pa	497 Pa	506 Pa
efficiency	53.1%	53.0%	53.7%

achieved the design goal and effectively solved the noise problem.

Compared with previous studies, this study not only focused on the optimization of fan noise performance, but also pays more attention to reducing noise while maintaining high efficiency through the simultaneous comparison of simulation and experiment. The efficiency requirements of traditional automobile radiator fans were generally not high, and the design focused on optimizing blade shape and changing materials to optimize noise. Although noise reduction solutions have been proposed, they often sacrifice some fan performance.[21,22] This study successfully achieved noise reduction and improved performance through the innovative design of non-uniformly arranged blades and leading triangles, filling this research gap.

These research results not only verify the effectiveness of innovative designs in reducing fan noise, but also provide new ideas and methods for fan design, which is of great significance to related industrial applications, i.e., application scenarios that require efficient cooling and are sensitive to noise, such as new energy vehicles, computer cooling systems, and household appliances, the design scheme of this study has significant application value.

REFERENCES

[1] Lowson, M. V., Reduction of compressor noise radiation. *Journal of the Acoustics Society of America*, 1968; **43**:37–50. https://doi.org/10.1121/1.1910760

[2] Mellin, R.C., Sovran, G., Controlling the tonal characteristics of the aerodynamic noise generated by fan rotors. *Journal of Basic Engineering* 1970; **92**:143–54. https://doi.org/10.1115/1.3424923

[3] Ewald, D., Pavlovic, A., Bollinger, J.G., Noise reduction by applying modulation principles. *Journal of the Acoustics Society of America* 1971; **49**:1381–5. https://doi.org/10.1121/1.1912513

[4] Wright, S.E., Sound radiation from a lifting rotor generated by asymmetric disc loading, *Journal of Sound and Vibration* 1969; **9**:223–240. https://doi.org/10.1016/0022-460X(69)90029-7

[5] Sun, X.F., Study of aerodynamic acoustic characteristics of wind turbines with unequal pitch arrangement of blades. *Journal of Beijing Institute of Aeronautics and Astronautics* 1986; N4:137–145.

[6] Lewy S., Theoretical study of the acoustic benefits of an open rotor with uneven blade spacings. *Journal of the Acoustics Society of America* 1992; **92**:2181-5. https://doi.org/10.1121/1.405212

[7] Zhang, F., Wu, P., Wu, D.Z., Study on pressure fluctuation and fluctuation reduction of a micro vortex pump. *ASME 2014 Fluids Engineering Division Summer Meeting*, Chicago, USA. p. 1–8. https://doi.org/10.1115/FEDSM2014-21884

[8] Zhang, L., Wu, P., Wu, D.Z., Analyses of pressure fluctuation and fluctuation reduction of an automobile fuel pump. *ASME 2016 Fluids Engineering Division Summer Meeting*, Washington DC, USA. p. 1–9. https://doi.org/10.1115/FEDSM2016-7820

[9] Wright, T., Simmons, W. E., Blade sweep for low- speed axial fans. *ASME J. of Turbomachinery*, 1990; **112**(2):151–158. https://doi.org/10.1115/1.2927413

[10] Ouyang, H., Li, Y., Liu, J., Du, Z.-H., Internal flow mechanism and experimental research of low-pressure axial fan with forward-skewed blades. *Journal of Hydrodynamics, Ser. B*, **20**(3), 299–305 (2008). https://doi.org/10.1016/S1674-4770(08)60048-5

[11] Cai, N., Xu, J., Aerodynamic-Aeroacoustics performance of parametric effects for skewed-swept rotor. *Proceedings of the ASME Turbo Expo 2001: Power for Land, Sea, and Air*, New Orleans, LA, USA, June 4–7, 2001, Paper No. GT2001-0354. *ASME Digital Collection*. (2001) https://doi.org/10.1115/2001-GT-0354

[12] Jiang, B., Tonal noise reduction by unevenly spaced blades in a forward-curved-blades centrifugal fan. *Applied Acoustics* 2019; **146**:172–183. https://doi.org/10.1016/j.apacoust.2018.11.007

[13] Lai, Y., Weng, C., Lu, Y., Karlsson, M., Abom, M., Knutsson, M., Study of Installation Effects on Automotive Cooling Fan Noise. *SAE International Journal of Advances and Current Practices in Mobility* 2022; **5**(2):803–809. https://doi.org/10.4271/2022-01-0935

[14] Yadegari, M., Ommi, F., Aliabadi, S. K., Saboohi, Z., Reducing the Aerodynamic Noise of the Axial Flow Fan with Perforated Surfaces, *Applied Acoustics*, **215**, 109720, 2023. https://doi.org/10.1016/j.apacoust.2023.109720

[15] Lighthill, M.J., On sound generated aerodynamically I. General theory. Proceedings of the Royal Society 1952; A211:564-587. https://doi.org/10.1098/rspa.1952.0060

[16] Ffowcs Williams, J. E., Hawkings, D. L., Sound Generation by Turbulence and Surfaces in Arbitrary Motion. *Philosophical Transactions of the Royal Society of London. Series A, Mathematical and Physical Sciences* 1969; A264(1151):321-342. https://doi.org/10.1098/rsta.1969.0031

[17] *ISO 5801: Fans – Performance testing using standardized airways*. 2017.

[18] G. M. Lilley. A study of the silent flight of the owl. *AIAA* 1998-2340, 1998. https://doi.org/10.2514/6.1998-2340

[19] Bachmann, T., Klan, S., Baumgartner, W., Klaas, M., Schroder, W., Wagner, H., Morphometric characterization of wing feathers of the barn owl Tyto alba pratincola and the pigeon Columba livia. *Frontiers in Zoology* 2007, **4**(23): 1–15. https://doi.org/10.1186/1742-9994-4-23

[20] Sarradj, E., Fritzsche, C., Geyer., T., Silent owl flight: bird flyover noise measurements. *AIAA Journal 2011*, **49**(4): 769–779. https://doi.org/10.2514/1.J050703

[21] Cattanei, A., Ghio, R., Bongiovì, A., Reduction of the tonal noise annoyance of axial flow fans by means of optimal blade spacing. *Applied Acoustics*, **68**(11–12), 1323–1345 (2007). https://doi.org/10.1016/j.apacoust.2007.01.004

[22] Qingyi, S., Haodong, X., Jian, C., Jiangtao, Z., (2023). Experimental and numerical study on a new noise reduction design for a small axial fan. *Applied Acoustics, 211*, 109535. https://doi.org/10.1016/j.apacoust.2023.109535